CHEMISTRY
A EUROPEAN JOURNAL

DOI: 10.1002/chem.200800487

# Metallaboranes of the Early Transition Metals: Direct Synthesis and Characterization of $[\{(\eta^5\text{-}C_5Me_5)Ta\}_2B_nH_m]$ ($n=4$, $m=10$; $n=5$, $m=11$), $[\{(\eta^5\text{-}C_5Me_5)Ta\}_2B_5H_{10}(C_6H_4CH_3)]$, and $[\{(\eta^5\text{-}C_5Me_5)TaCl\}_2B_5H_{11}]$

**Shubhankar Kumar Bose,[a] K. Geetharani,[a] Babu Varghese,[b] Shaikh M. Mobin,[c] and Sundargopal Ghosh*[a]**

*Dedicated to Professor Ken Wade on the occasion of his 75th birthday*

**Abstract:** Reaction of $[Cp^*TaCl_4]$ ($Cp^*=\eta^5\text{-}C_5Me_5$) with a sixfold excess of $LiBH_4{\cdot}thf$ followed by $BH_3{\cdot}thf$ in toluene at 100 °C led to the isolation of hydrogen-rich metallaboranes $[(Cp^*Ta)_2B_4H_{10}]$ (**1**), $[(Cp^*Ta)_2B_5H_{11}]$ (**2**), $[(Cp^*Ta)_2B_5H_{10}(C_6H_4CH_3)]$ (**3**), and $[(Cp^*TaCl)_2B_5H_{11}]$ (**4**) in modest yield. Compounds **1**–**3** are air- and moisture-sensitive but **4** is reasonably stable in air. Their structures are predicted by the electron-counting rules to be a bicapped tetrahedron (**1**), bicapped trigonal bipyramids (**2**, **3**), and a *nido* structure based on a *closo* dodecahedron (**4**). Yellow tantalaborane **1** has a *nido* geometry with $C_{2v}$ symmetry and is isostructural with $[(Cp^*M)_2B_4H_8]$ (M = Cr and Re); whereas **2** and **3** are $C_{3v}$-symmetric and isostructural with $[(Cp^*M)_2B_5H_9]$ (M = Cr, Mo, W) and $[(Cp^*ReH)_2B_5Cl_5]$. The most remarkable feature of **4** is the presence of a hydride ligand bridging the ditantalum center to form a symmetrical tantalaborane cluster with a long Ta–Ta bond (3.22 Å). Cluster **4** is a rare example of electronically unsaturated metallaborane containing four TaHB bonds. All these new metallaboranes have been characterized by mass spectrometry, $^1H$, $^{11}B$, and $^{13}C$ NMR spectroscopy, and elemental analysis, and the structural types were unequivocally established by crystallographic analysis of **1**–**4**.

**Keywords:** boranes · boron · cluster compounds · metallaboranes · tantalum

## Introduction

Metallaborane chemistry is an interesting and diverse area of cluster chemistry that is closely allied to both polyhedral metal compounds and boron hydrides.[1–8] Although it continues to be a topic of intense research, development in this area has been slow,[1,3,5,9,10] partly due to the lack of convenient high-yield synthetic methods. Synthetic methods for the generation of transition-metal cluster compounds have historically been based around conditions that favor more stable products.[11] The development of metallaborane chemistry has followed a similar pathway, and new species are often isolated under conditions that favor the thermodynamic product, either through thermolysis or by simple metathesis reactions between a preformed polyborane anion and transition-metal halides.[3a–b,12]

Fehlner et al. have studied reactions between cyclopentadienyl transition-metal halides $[Cp^*MCl_n]$ ($Cp^*=\eta^5\text{-}C_5Me_5$) and monoborane reagents $BH_3{\cdot}thf$, $LiBH_4{\cdot}thf$, and $BHCl_2{\cdot}SMe_2$,which often afford metallaboranes (M = Cr,[13] Mo,[14] W,[15] Re,[16] Ru,[17] Co,[18] Rh,[19] and Ir.[20]) in modest to high yield under mild conditions. However, a different situation arises in the case of early transition-metal complexes $[Cp^*MCl_n]$, (M = V, Nb, or Ta), which are generally more reactive towards monoborane reagents. Despite the availability of well-developed routes to metallaboranes of Group 6–9 metals, to our knowledge examples of characterized Group 5 metallaboranes are very rare.[21] Tantalaboranes $[(Cp^*Ta)_2(B_2H_6)_2]$[22] and $[(Cp^*Ta)Cl_2B_4H_8]$[23] were synthe-

---

[a] S. K. Bose, K. Geetharani, Dr. S. Ghosh
Department of Chemistry
Indian Institute of Technology Madras
Chennai 600036 (India)
Fax: (+91) 44-2257-4202
E-mail: sghosh@iitm.ac.in

[b] Dr. B. Varghese
Sophisticated Analytical Instruments Facility
Indian Institute of Technology Madras
Chennai 600036 (India)

[c] S. M. Mobin
National Single Crystal X-ray Diffraction Facility
Indian Institute of Technology Bombay, Mumbai 400076 (India)

sized by using the same approach as described above, that is, the reaction between $LiBH_4$·thf or $BH_3$·thf and [Cp*$TaCl_4$]. As tantalaboranes are rare, and structurally characterized examples even more so, we reinvestigated the tantalum system by using more vigorous heating and an excess of $BH_3$·thf. Here we present the results of reactions between [Cp*$TaCl_4$] and $LiBH_4$·thf and $BH_3$·thf to afford tantalaboranes **1**–**4** in modest yield, all of which were characterized by spectroscopic methods and X-ray diffraction.

## Results and Discussion

**Synthesis of [(Cp*Ta)$_2$B$_4$H$_{10}$], [(Cp*Ta)$_2$B$_5$H$_{11}$], [(Cp*Ta)$_2$B$_5$H$_{10}$(C$_6$H$_4$CH$_3$)], and [(Cp*TaCl)$_2$B$_5$H$_{11}$]**: As shown in Scheme 1, reaction of [Cp*$TaCl_4$] with a sixfold excess of $LiBH_4$·thf followed by $BH_3$·thf in toluene at 100 °C results a mixture of [(Cp*Ta)$_2$B$_4$H$_{10}$] (**1**), [(Cp*Ta)$_2$B$_5$H$_{11}$] (**2**), [(Cp*Ta)$_2$B$_5$H$_{10}$(C$_6$H$_4$CH$_3$)] (**3**), and [(Cp*TaCl)$_2$B$_5$H$_{11}$] (**4**), which were separated by TLC.

**[(Cp*Ta)$_2$B$_4$H$_{10}$] (1)**: Compound **1** was characterized spectroscopically and by X-ray structure determination. The mass spectrometric data suggested a molecular formula of $C_{20}H_{40}Ta_2B_4$. In the absence of crystallographic data, the molecular formula of **1** and its spectroscopic properties best fit the structure shown in Scheme 1. By analogy with Cr and Re compounds, **1** can be considered as a 42-electron, electronically unsaturated dimetal compound with $B_2$ ligands bridging in a perpendicular fashion. The $^{11}$B NMR data (two resonances in 1:1 ratio) suggests a structure, if static, of higher symmetry. Consistent with this observation, **1** shows one kind of Cp* signal and two signals for six TaHB protons. Selective decoupling experiment showed that four of the six TaHB protons bridge the open four-membered face, while the other two are located on the boron atoms of the tetrahedral $Ta_2B_2$ core.

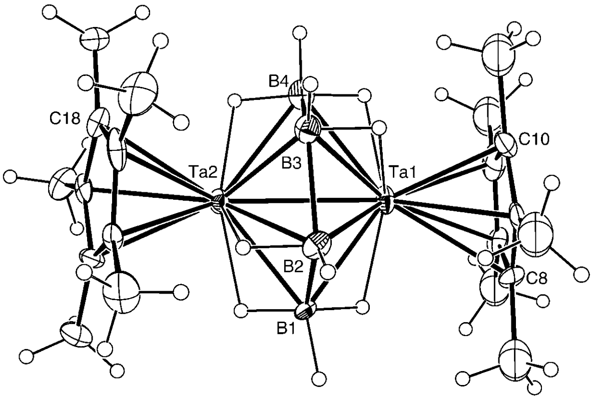

Figure 1. Molecular structure and labeling scheme for [(Cp*Ta)$_2$B$_4$H$_{10}$] (**1**). Selected bond lengths [Å] and angles [°]: Ta1–Ta2 2.8909(4), Ta1–B1 2.437(15), Ta1–B2 2.441(14), Ta1–B3 2.452(6), Ta1–B4 2.33(2), B1–B2 1.70(2), B2–B3 1.93(3), B3–B4 1.71(3), Ta2–B1 2.378(13), Ta2–B2 2.382(15), Ta2–B3 2.290(10), Ta2–B4 2.34(2); B2-Ta1-B3 46.4(6), B1-Ta1-B3 81.0(5), B4-Ta1-B1 103.3(5), B4-Ta2-B1 104.7(5), B3-Ta2-B4 43.2(6), C6-Ta1-B1 147.1(4).

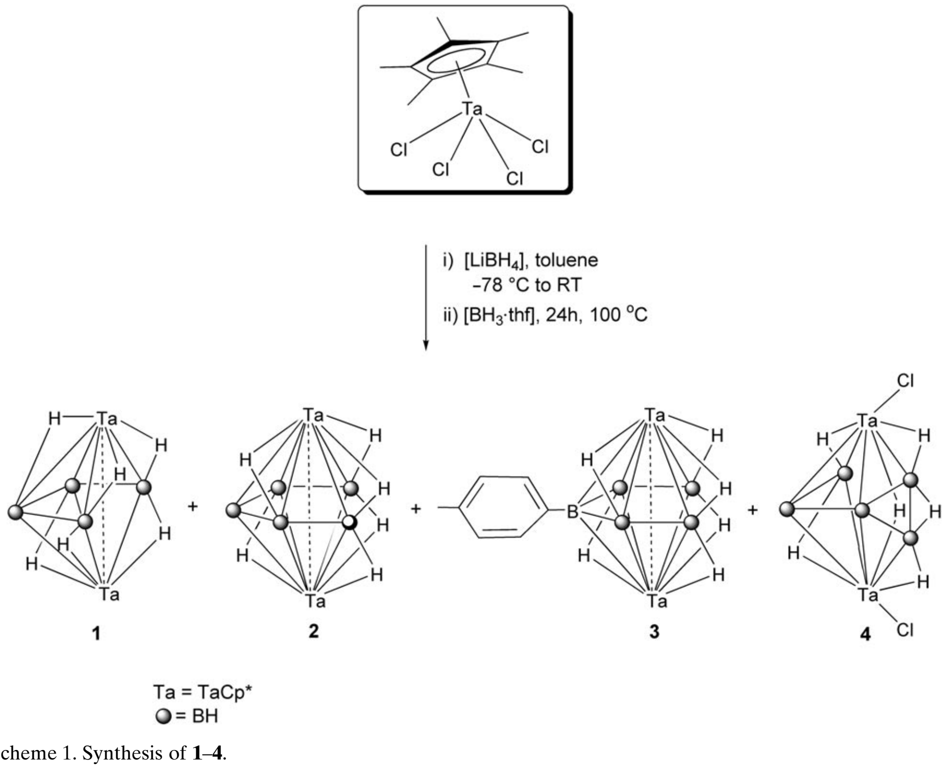

Scheme 1. Synthesis of **1**–**4**.

The spectroscopic data are consistent with the solid-state structure (Figure 1). Compound **1** is a dimetallatetrahedron capped on each $Ta_2B$ face by a $BH_3$ group such that extra four hydrogen atoms reside on the butterfly-shaped face generated by the $Ta_2B_2$ tetrahedron. On the basis of the capping principle[24] the skeletal electron count is determined by the central polyhedron (i.e., $Ta_2B_2$ tetrahedron) and amounts to five skeletal electron pairs (SEP), two electrons less than required for the bicapped tetrahedron. Thus, **1** does not obey the electron-counting rules[24–25] for the observed geometry.

The existence of compound **1** permits structural comparison with Cr and Re analogues without perturbations caused by additional metal fragments or ligands. The important geometrical differences among the bicapped tetrahedral cores of [(Cp*M)$_2$B$_4$H$_{8+n}$] (M = Cr, Re:

$n=0$; M=Ta: $n=2$) are shown in Figure 2 and Table 1. As the qualitative cluster shapes of [$(Cp^*Ta)_2B_4H_{10}$], [$(Cp^*Cr)_2B_4H_8$], and [$(Cp^*ReH_2)_2B_4H_4$] are the same, differences are sought in the magnitude of the structural parameters and the locations of the hydrogen atoms. The Ta–Ta and Re–Re distances of 2.89 and 2.81 Å are in the range observed for single bonds, whereas the Cr–Cr distance of 2.87 Å in [$(Cp^*Cr)_2B_4H_8$] is longer than a normal single-bond length.[13a] On the other hand, the increased average Ta–B distance (2.38 Å) and dihedral angle (167°) of the hydrogen-bridged butterfly may reflect the larger metal radius of Ta. Although the average B–B distance in **1** is similar, that between the two capping boron atoms of 3.68 Å is much wider than those of its Cr and Re analogues. The observed $^1H$ and $^{11}B$ NMR chemical shift correlation of **1** with Cr and Re analogues may be due to perturbation of the electronic environment of the boron atoms by the metal. On going from the lighter to the heavier metal atom, the $^1H$ (TaHB protons) and $^{11}B$ NMR (both capping and $M_2B_2$ tetrahedron boron atoms) resonances appear at low field (Table 1).

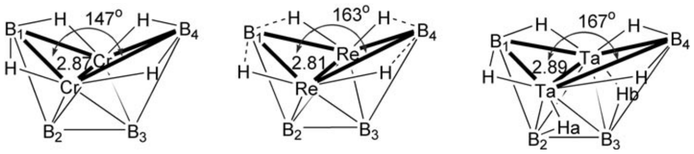

Figure 2. Geometric and chemical-shift differences between the cluster cores of [$(Cp^*M)_2B_4H_{8+n}$] (M=Cr, Re: $n=0$; M=Ta: $n=2$). Cp* ligands omitted for clarity.

Table 1. Selected structural parameters and $^1H$ and $^{11}B$ NMR chemical shifts of **1**, [$(Cp^*Cr)_2B_4H_8$], and [$(Cp^*ReH_2)_2B_4H_4$].

| Compound | SEP | $d_{M-M}$ [Å] | Av $d_{M-B}$ [Å] | Av $d_{B-B}$ [Å] | $d_{B-B}$ [Å][a] | Dihedral angle [°] ($M_2B_2$ tetrahedron) | $^1H$ NMR [ppm] (M-H-B) | $^{11}B$ NMR [ppm][c] |
|---|---|---|---|---|---|---|---|---|
| [$(Cp^*Cr)_2B_4H_8$] | 5 | 2.87 | 2.06 | 1.70 | 3.02 | 147.6 | −3.90 | 34.3, 126.5 |
| [$(Cp^*ReH_2)_2B_4H_4$] | 6 | 2.81 | 2.17 | 1.77 | 3.20 | 163.4 | −11.52 | 1.30, 68.7 |
| [$(Cp^*Ta)_2B_4H_{10}$] (**1**) | 5 | 2.89 | 2.38 | 1.78 | 3.68 | 167.7 | −7.23, −3.88[b] | 0.3, 16.6 |

[a] Distance between capping boron atoms B1 and B4 (Figure 2) in the open face of bicapped tetrahedral structure. [b] Two TaHB protons ($H_a$ and $H_b$ as shown in Figure 2) in $Ta_2B_2$ tetrahedral core. [c] Two sets of $^{11}B$ resonances (B1 and B4; B2 and B3) in the bicapped $M_2B_4$ tetrahedron.

**[$(Cp^*Ta)_2B_5H_{11}$] (2)**: Compound **2** was isolated by TLC in modest yield. The NMR spectra imply a diamagnetic compound. The mass spectrum of **2** is consistent with a formula containing two Ta and five B atoms, and the parent-ion mass corresponds to addition of a BH unit to [$(Cp^*Ta)_2B_4H_{10}$] (**1**). This formulation of **2** rationalizes the presence of three $^{11}B$ NMR resonances in 2:2:1 ratio. The $^{11}B$ NMR data indicate the presence of two pairs of equivalent boron atoms and a unique boron atom, all linked directly to single hydrogen atoms. In one pair (open face) each boron atom is bonded to two bridging hydrogen atoms, and in the other each boron atom is bonded to one bridging hydrogen atom. Furthermore, $^1H$ and $^{13}C$ NMR spectra imply two equivalent Cp* ligands. Consistent with empirical observations,[26] the signal of one pair (B2 and B4 in Figure 3) is found at low field, whereas those of the other (B1 and B5) lie within the range typical of boranes.

The single-crystal X-ray diffraction structure of **2** (Figure 3) confirms the structural inferences made on the basis of spectroscopic data. Superficially this geometry resembles a hexagonal bipyramid with a single missing equatorial vertex but, given the electron count of six SEP, is probably more accurately thought of as a bicapped trigonal bipyramid. A similar structural interpretation has been suggested for [$(Cp^*M)_2B_5H_9$] (M=Cr,[13b,27] Mo,[13b,14,27,28] W[15]) and [$(Cp^*ReH)_2B_5Cl_5$],[29] and in each case the trigonal-bipyramidal $M_2B_3H_3$ unit is capped by two $BH_3$ fragments over the $M_2B$ faces. Such an interpretation implies the presence of a Ta–-Ta single bond, and the bond length of 2.92 Å is consistent with this.[30] Comparing the structural parameters and chemical shift of **2** are with those of Cr, Mo, W, and Re analogues (Table 2) reveals several contrasting features. Not only is the M–M distance significantly longer in **2**, but the average M–B and B–B distances are also noticeably longer. Differences in Ta–B and B–B distances can be accounted for by the larger size of the Ta center and two extra bridging hydrogen atoms compared to the case of Cr.[31] The distance between the two capping boron atoms differ slightly with respect to the size of the open face of the cluster, which is more open in the Ta system. Although differences in $^1H$ chemical shift of the

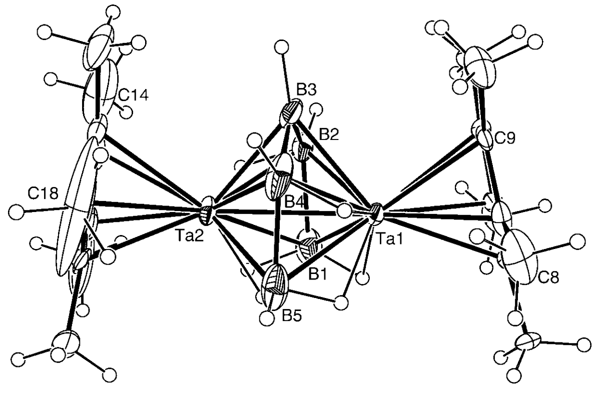

Figure 3. Molecular structure and labeling scheme for [$(Cp^*Ta)_2B_5H_{11}$] (**2**). Selected bond lengths [Å] and angles [°]: Ta1–Ta2 2.9261(4), Ta1–B1 2.263(13), Ta1–B3 2.268(11), Ta1–B2 2.294(11), Ta1–B4 2.333(11), Ta1–B5 2.435(12), Ta2–B2 2.348(11), Ta2–B1 2.452(12), Ta2–B3 2.264(13), Ta2–B4 2.291(11), Ta2–B5 2.314(13), B1–B2 1.838(18), B2–B3 1.751(19), B3–B4 1.77(2), B4–B5 1.86(2); B1-Ta1-B3 86.3(5), B1-Ta1-B4 104.7(4), B2-Ta1-B4 84.4(5), B3-B2-B1 119.3(9), B1-B2-Ta1 65.3(6).

Table 2. Selected structural parameters and $^1$H and $^{11}$B NMR chemical shifts of $[(Cp^*M)_2B_5H_{9+n}]$ (M = Cr, Mo, W; $n = 0$; M = Ta: $n = 2$).

| Compound | SEP | $d_{M-M}$ [Å] | Av $d_{M-B}$ [Å] | Av $d_{B-B}$ [Å] | $d_{B-B}$ [Å][a] | $^1$H NMR [ppm] (M-H-B) | Angle [°] between Cp* | $^{11}$B NMR [ppm][c] |
|---|---|---|---|---|---|---|---|---|
| $[(Cp^*Ta)_2B_5H_{11}]$ (**2**) | 6 | 2.92 | 2.32 | 1.80 | 3.21 | −6.6 and −3.8[b] | 20 | 3.7, 23.9, 44.7 |
| $[\{Cp^*Ta\}_2B_5H_{10}L]$ (**3**) ($L = C_6H_4CH_3$) | 6 | 2.90 | 2.32 | 1.80 | 3.19 | na[d] | 13 | na[d] |
| $[(Cp^*Cr)_2B_5H_9]$ | 6 | 2.62 | 2.15 | 1.67 | 3.08 | −6.20 | 23 | 25.0, 91.5, 86.2 |
| $[(Cp^*Mo)_2B_5H_9]$ | 6 | 2.80 | 2.24 | 1.72 | 3.22 | −6.99 | 31 | 62.9[e] (3B), 25.8 |
| $[(\eta^5\text{-}C_5H_4MeMo)_2B_5H_9]$ | 6 | 2.81 | 2.25 | 1.73 | 3.26 | −7.01 | 30 | 61.6, 27.8, 59.7 |
| $[(Cp^*W)_2B_5H_9]$ | 6 | 2.81 | 2.23 | 1.71 | 3.16 | −8.20 | 27 | 26.8, 46.9, 49.2 |
| $[(Cp^*ReH)_2B_5Cl_5]$ | 6 | 2.76 | 2.20 | 1.74 | 2.85 | −9.30 | 13 | 48.3, 88.3, 28.1[f] |

[a] Nonbonding distance between the two capping boron atoms (B1 and B5 in Figure 3). [b] Two equivalent TaHB protons (Ta1HB4 and Ta2HB2) in $Ta_2B_3$ trigonal bipyramid. [c] Three $^{11}$B resonances: capping (B1 and B5), apical (B2 and B4), and the unique equatorial boron atom (B3) in $M_2B_5$ bicapped trigonal-bipyramidal core. [d] na = not available. Identification of **3** is based solely on solid-state structure determination. [e] Accidental overlap of the capping and equatorial $^{11}$B resonances. [f] All five terminal hydrogen atoms are substituted by chlorine atoms.

MHB potons in $[(Cp^*M)_2B_5H_{9+n}]$ (M = Cr, Mo, W: $n = 0$; M = Ta: $n = 2$) are not noticeable, there is a large difference in $^{11}$B chemical shift of three types of boron atoms in the $M_2B_3$ core on moving from first- to third-row transition metal.

**$[\{Cp^*Ta\}_2B_5H_{10}(C_6H_4CH_3)]$ (3)**: Identification of **3** is based solely on solid-state structure determination of a crystal selected from a mixture of **2** and **3**. The molecular structure of **3** (Figure 4) is similar to that of **2**, that is, bicapped trigonal bipyramid, except that one of the terminal BH hydrogen atoms has been replaced by a $C_6H_4Me$ group. As expected, the distances and angles are similar to those found in **2** (Table 2).

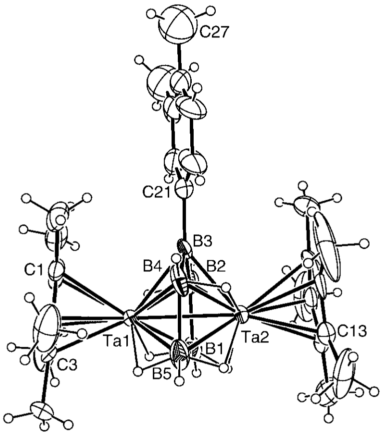

Figure 4. Molecular structure and labeling scheme for $[\{Cp^*Ta\}_2B_5H_{10}(C_6H_4CH_3)]$ (**3**). Selected bond lengths [Å] and angles [°]: Ta1–Ta2 2.9099(12), Ta1–B1 2.409(15), Ta1–B3 2.325(11), Ta1–B2 2.317(13), Ta1–B4 2.345(9) Ta1–B5 2.279(14), Ta2–B2 2.238(13), Ta2–B1 2.318(14), Ta2–B3 2.278(13), Ta2–B4 2.393(9), Ta2–B5 2.406(14), B1–B2 1.821(19), B2–B3 1.774(18), B3–B4 1.79(2), B4–B5 1.89(2); B3-Ta1-B1 84.0(4), B2-Ta1-B1 45.3(5), B4-Ta1-B1 103.5(4), B3-B2-B1 123.5(10), Ta1-B2-Ta2 79.4(4).

The ORTEP representation of **3** shows large librational motion with Ta1–Ta2 as a librational axis. The $p$-tolyl $CH_3$ group is disordered over two positions, each with 50% occupancy. The main phenyl plane of the tolyl is inclined to the Cp* planes by 10.9(6)° (C1–C5) and 9.7(6)° (C11–C15). Strong C–H⋅⋅⋅π interactions between the phenyl plane of the tolyl moiety and H8A of the methyl group (H8A_1⋅⋅⋅π 2.670(19) Å, symmetry_1: $1+x$, $-1+y$, $z$) form one-dimensional zigzag chains in the crystal lattice. The packing is further stabilized through intermolecular van der Waals interactions among hydrogen atoms. All the boron atoms (B1–B5) lie almost in an ideal plane, with a maximum deviation of 0.022(9) Å for B2, that perpendicularly bisects the Ta–Ta axis.

Several attempts to synthesize **3** by using the same approach as for **2**, which involves $BH_3$·thf and $LiBH_4$·thf as boron sources and toluene as solvent, failed. Thus, information on the origin of **3** must await additional detailed work, including characterization of intermediate products.

**$[(Cp^*TaCl)_2B_5H_{11}]$ (4)**: Compound **4** was isolated in modest yield and was characterized spectroscopically and by X-ray diffraction. The mass spectrum shows a molecular-ion peak at $m/z$ 767 corroborating the composition of $C_{20}H_{41}Ta_2B_5Cl_2$, and the $^{11}$B NMR spectrum (temperature-independent down to −55 °C) exhibits four doublets in intensity ratio of 1:1:1:2, consistent with a symmetric structure or a fluxional system. Besides the BH protons (1:1:1:2), one TaHTa, one BHB, and four TaHB protons are also observed. A $^1$H/$^{11}$B HETCOR experiment showed two of the four TaHB protons to be coupled exclusively to a pair of equivalent boron atoms and the other two to the unique boron atom (open face).

The framework geometry of **4** (Figure 5), which is unexpected for a tantalaborane, only became clear when the solid state structure was determined. It is a *nido* structure based on a *closo* dodecahedron. The average B–B distance (1.76 Å) is comparable with those in **1**, **2**, and others,[21a,23] but the average Ta–B (2.38 Å) and Ta–Ta (3.22 Å) distances are about 0.1 and 0.3 Å longer. The Ta–Ta distance is too long for a full Ta–Ta single bond (cf. $[\{TaCp^*Cl_2H\}_2]$[30]), but it is too short to propose that there is no significant interaction at all between the two metal centers.[32] Another interesting feature is the presence of a bridging hydride ligand between the two Ta centers. Usually, a bridging hydride ligand pulls the metal atoms together to form a three-

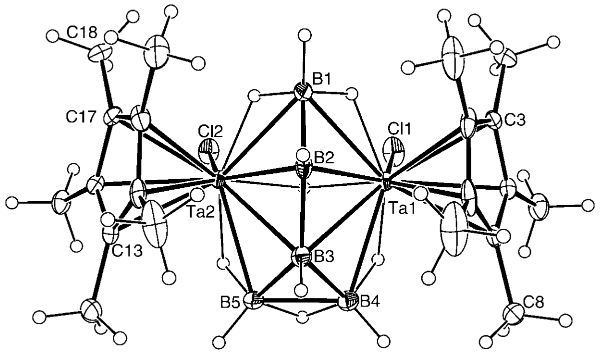

Figure 5. Molecular structure and labeling scheme for [$(Cp^*TaCl)_2B_5H_{11}$] (**4**). Selected bond lengths [Å] and angles [°]: Ta1–Ta2 3.2219(3), Ta1–B2 2.258(7), Ta1–B3 2.440(7), Ta1–B1 2.413(7), Ta1–B4 2.422(8), Ta2–B2 2.279(7), Ta2–B1 2.403(8), Ta2–B3 2.431(7), Ta2–B5 2.431(7), B1–B2 1.732(11), B2–B3 1.734(10), B3–B5 1.770(11), B3–B4 1.773(10), B4–B5 1.832(10); B2-Ta1-B1 43.4(3), B(2)-Ta(1)-Ta(2) 45.02(18), B1-Ta1-Ta2 47.89(18), B4-Ta1-Ta2 73.38(18).

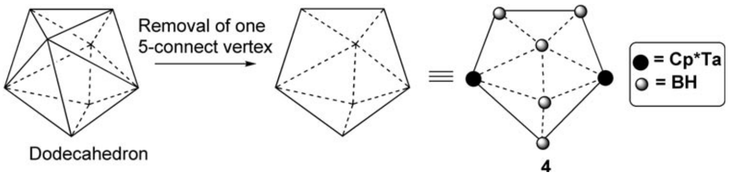

Figure 6. Generating the structure of **4** by removing one five-connected vertex of a dodecahedron.

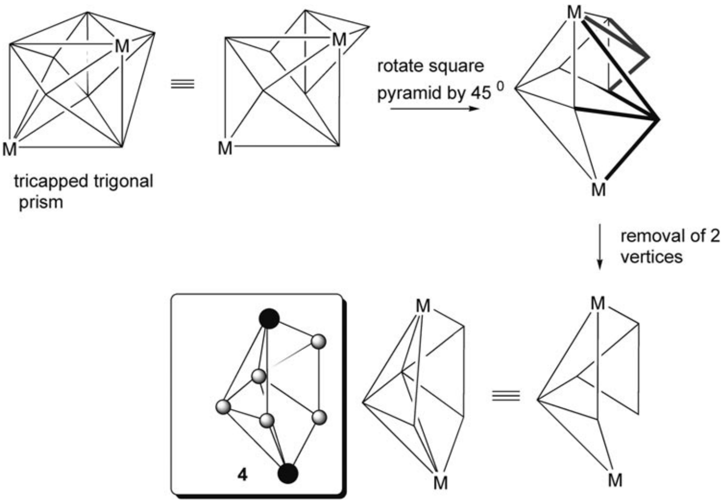

Figure 7. Generating the structure of **4** by 45° rotation of one of the square pyramidal faces of a tricapped trigonal prism around its $C_2$ axis followed by removal of two vertices.

center, two-electron bond,[33] but this is in marked contrast to [$(Cp^*TaCl)_2B_5H_{11}$], in which the M–M distance is too large for a significant binding interaction (Ta–Ta 3.22 Å). All the non-Cp* hydrogen atoms were found during refinement including four TaHB, one TaHTa, and one BHB.

The $^1$H and $^{11}$B NMR spectra are consistent with the solid-state X-ray structure of [$(Cp^*TaCl)_2B_5H_{11}$] (**4**), which rationalizes the presence of four $^{11}$B resonances in the ratio of 1:1:1:2. The signal of relative intensity 2:1 at $\delta = 18.8$ and 15 ppm can be assigned to the pair of equivalent boron atoms and the unique boron atom, respectively. The other two resonances of relative intensity 1:1 at $\delta = 77.7$ and $-10$ ppm can be assigned to the unique four- and five-connected boron atoms, respectively. The two pairs of equivalent TaHB and one BHB hydrogen atoms can be placed as shown in Scheme 1. The hydride ligands can be observed by NMR or IR spectroscopy.[30,32c,34] In the $^1$H NMR spectrum of **4** a hydride resonance with an integrated area of unity relative to each $C_5Me_5$ group is found at $\delta = 8.55$ ppm. The spectrum does not change on cooling or heating the sample. Based on the $^1$H NMR data of other tantalum hydrides,[30,34] this chemical shift was assigned for the TaHTa bridging hydrogen atom. In the IR spectrum a medium-strength, broad peak at 1556 $cm^{-1}$ can be assigned to a metal hydride mode. Although the position of the peak is consistent with bridging hydride ligands, the possibility that the hydride is terminally bound cannot be excluded by this IR data alone.

The crystal structure of **4** (Figure 5) can be interpreted as a *nido* cluster formally derived from an eight- or nine-vertex deltahedron. The former case gives a *nido* cluster simply by removing one five-connected vertex of a dodecahedron (Figure 6). Alternatively, the observed geometry of **4** may also be generated by 45° rotation of one of the square pyramidal faces of a tricapped trigonal prism around its $C_2$ axis followed by removal of two vertices (Figure 7). The skeletal electron count for such a molecule is eight pairs (if we take [Cp*TaCl] as zero-electron), one pair short of the nine required for a dodecahedral geometry. Cluster **4** is therefore electronically unsaturated.

## Conclusion

Although reactions of monocyclopentadienylmetal halides [$CpMX_n$] with nucleophiles have been extensively investigated in general,[35] reaction with electrophiles has received comparatively less attention to date. A new synthetic route to [$(Cp^*Ta)_2B_nH_m$] ($n = 4$, $m = 10$; $n = 5$, $m = 11$) clusters has been developed by the reaction of [$Cp^*TaCl_4$] with the electrophiles $LiBH_4$·thf and $BH_3$·thf. This route provided access to metallaboranes of earlier transition metals and yielded a variety of structural types, some of which have novel cage geometries and other structural features. Our results for this Ta system, as well as other related systems,[36] suggest that the metal fragment provides an electron-rich site for electrophilic attack and thus promotes addition of $BH_3$ to metallaborane clusters. Cluster **4** is a novel type of unsaturated ditantalaborane cluster, and its thermodynamic stability, together with its stability in air, makes it unique. The synthesis and ongoing investigation of the chemistry of **2**, with particular emphasis on the synthesis of higher tantalaboranes by stepwise building-block approaches, as in the synthesis of rhenaboranes[29] and ruthenaboranes,[37] is an exciting development in the little-investigated area of metallaborane chemistry of early transition metals and may allow the rational development of new materials.

## Experimental Section

**General procedures and instrumentation**: All operations were conducted under an Ar/$N_2$ atmosphere by standard Schlenk techniques. Solvents were distilled prior to use under argon. [Cp*$TaCl_4$], $BH_3$·thf, and $LiBH_4$·thf (Aldrich) were used as received. [$Bu_4N(B_3H_8)$] as external reference for $^{11}$B NMR spectroscopy was synthesized by the literature method.[38] TLC was performed on aluminum-supported silica gel TLC plates (∅ 250 mm, Merck TLC Plates). NMR spectra were recorded on 400 and 500 MHz Bruker FT NMR spectrometers. Residual solvent protons were used as reference for $^1$H NMR ($\delta$([$D_6$]benzene) = 7.15 ppm), while a sealed tube containing [$Bu_4N(B_3H_8)$] in [$D_6$]benzene ($\delta_B$ = −30.07 ppm) was used as external reference for the $^{11}$B NMR spectra. IR spectra were recorded on a Nicolet 6700 FT spectrometer. Mass spectra were obtained on a JEOL JMS-AX505HA mass spectrometer with perfluorokerosene as standard and a Jeol SX 102/Da-600 mass spectrometer with argon/xenon (6 kV, 10 mÅ) as FAB gas.

**General procedure for synthesis of [$(Cp^*Ta)_2B_nH_m$ ]($n$=4, $m$=10; $n$=5, $m$=11), [$(Cp^*Ta)_2B_5H_{10}(C_6H_4Me)$] and [$(Cp^*TaCl)_2B_5H_{11}$]**: In a flame-dried Schlenk tube [Cp*$TaCl_4$] (0.12 g, 0.26 mmol) was suspended in toluene (15 mL) and cooled to −78 °C, $LiBH_4$·thf (0.8 mL, 1.56 mmol) was added by syringe, and the reaction mixture was warmed slowly over 30 min to room temperature and left stirring for an additional hour. The solvent was evaporated under vacuum, the residue was extracted into hexane, and filtration afforded an extremely air and moisture sensitive deep blue intermediate. The filtrate was concentrated, and a toluene solution (20 mL) of the intermediate was pyrolyzed in the presence of an excess of $BH_3$·thf at 100 °C for 24 h. The solvent was dried and the residue was extracted into hexane and passed through Celite. After removal of solvent, the residue was subjected to chromatographic workup on silica-gel TLC plates. Elution with hexane/$CH_2Cl_2$ (80/20) yielded three bands. The first, red band was a mixture of [$(Cp^*Ta)_2B_5H_{11}$] (**2**) and [$(Cp^*Ta)_2B_5H_{10}(C_6H_4Me)$] (**3**), the second, yellow band was [$(Cp^*Ta)_2B_4H_{10}$] (**1**; 0.014 g, 8 %), and the third, red band was [$(Cp^*TaCl)_2B_5H_{11}$] (**4**; 0.027 g, 14 %). X-ray-quality crystals of **1**–**4** were grown by slow diffusion of hexane at 2 °C.

Spectroscopic data for [$(Cp^*Ta)_2B_4H_{10}$] (**1**): $^{11}$B NMR (400 MHz, [$D_6$]benzene, 22 °C): $\delta$ = 16.6 (s, 2B), 0.3 ppm (s, 2B); $^1$H NMR (400 MHz, [$D_6$]benzene, 22 °C): $\delta$ = 6.02 (partially collapsed quartet (pcq); 2$BH_t$), 4.37 (pcq; 2$BH_t$), 2.11 (s, 30H; Cp*), −3.88 (br; 2TaHB), −7.23 ppm (pcq, 4TaHB); $^{13}$C NMR (500 MHz, [$D_6$]benzene, 22 °C): $\delta$ = 110.8 (s; $C_5Me_5$), 11.2 ppm (s; $CH_3$ in $C_5Me_5$); IR (hexane): $\tilde{\nu}$ = 2455 cm$^{-1}$ (w, $BH_t$); MS (FAB) P$^+$(max): $m/z$ (%): 684 (isotopic pattern for 2Ta and 4B atoms); elemental analysis calcd (%) for $^{12}C_{20}{}^1H_{40}{}^{11}B_4{}^{170}Ta_2$: C 35.03, H 5.88; found: C 36.12, H 6.01.

Spectroscopic data for [$(Cp^*Ta)_2B_5H_{11}$] (**2**): $^{11}$B NMR (400 MHz, [$D_6$]benzene, 22 °C): $\delta$ = 44.8 (s, 1B), 23.9 (s, 2B), 3.7 ppm (s, 2B); $^1$H NMR (400 MHz, [$D_6$]benzene, 22 °C): $\delta$ = 5.43 (pcq; 2$BH_t$), 4.39 (pcq; 2$BH_t$), 3.14 (pcq; 1$BH_t$), 2.16 (s, 30H; Cp*), −3.93 (br; 2TaHB), −6.65 ppm (pcq; 4TaHB); $^{13}$C NMR (500 MHz, [$D_6$]benzene, 22 °C): $\delta$ = 110.8 (s; $C_5Me_5$), 12.9 ppm (s; $CH_3$ in $C_5Me_5$); IR (hexane): $\tilde{\nu}$ = 2455 (w), 2496 cm$^{-1}$ (w, $BH_t$); MS (FAB) P$^+$(max): $m/z$(%): 696 (isotopic pattern for 2Ta and 5B atoms); elemental analysis calcd (%) for $^{12}C_{20}{}^1H_{41}{}^{11}B_5{}^{170}Ta_2$: C 34.44, H 5.92; found: C 35.77, H 6.22.

Spectroscopic data for [$(Cp^*TaCl)_2B_5H_{11}$] (**4**): $^{11}$B NMR (400 MHz, [$D_6$]benzene, 22 °C): $\delta$ = 77.7 (s, 1B), 18.8 (s, 2B), 15.1 (s, 1B), −10.0 ppm (s, 1B); $^1$H NMR (400 MHz, [$D_6$]benzene, 22 °C): $\delta$ = 8.58 (s; 1TaHTa), 4.18 (pcq; 2$BH_t$), 3.80 (pcq; 1$BH_t$), 2.91 (pcq; 1$BH_t$), 2.82 (pcq; 1$BH_t$), 1.87 (s, 30H; Cp*), −0.06 (br; 1BHB), −2.38 (br; 2TaHB), −2.76 ppm (br, 2TaHB); $^{13}$C NMR (500 MHz, [$D_6$]benzene, 22 °C): $\delta$ = 116.8 (s; $C_5Me_5$), 14.4 (s; $CH_3$ in $C_5Me_5$); IR (hexane): $\tilde{\nu}$ = 2441 (w), 2490 cm$^{-1}$ (w, $BH_t$); MS (FAB) P$^+$(max): $m/z$ (%): 767 (isotopic pattern for 2Ta, 2Cl, and 5B atoms); elemental analysis calcd (%) for $^{12}C_{20}{}^1H_{41}{}^{11}B_5{}^{170}Ta_2{}^{37}Cl_2$: C 31.26, H 5.38; found: C 33.02, H 6.32.

**X-ray structure determination**: Diffraction data for **1**, **2**, and **4** were collected and integrated by using an Oxford Diffraction XCALIBUR-S CCD system equipped with graphite-monochromated Mo$_{K\alpha}$ radiation ($\lambda$ = 0.71073 Å) at 150 K. Crystal data for **3** were collected and integrated on a Bruker AXS KAPPA APEX2 CCD diffractometer with graphite-monochromated Mo$_{K\alpha}$ ($\lambda$ = 0.71073 Å) radiation at 293 K. The structures were solved by heavy-atom methods using SHELXS-97 or SIR92 (Altornare et al., **1993**) and refined using SHELXL-97 (G.M. Sheldrick, University of Göttingen).

[$(Cp^*Ta)_2B_4H_{10}$] (**1**): $C_{20}H_{40}B_4Ta_2$, monoclinic, $C2$, $a$ = 18.9197(3), $b$ = 13.8180(3), $c$ = 9.5639(2) Å, $\beta$ = 93.987(2)°, $Z$ = 4, $\rho_{calcd}$ = 1.826 Mg m$^{-3}$, final $R$ indices [$I > 2\sigma(I)$] $R_1$ = 0.0481, $wR_2$ = 0.1118, index ranges $-27 \le h \le 28$, $-20 \le k \le 20$, $-14 \le l \le 13$, crystal size 0.23 × 0.21 × 0.17 mm, reflections collected 17962, independent reflections 7260, ($R$(int) = 0.0461), GOF on $F^2$ 1.025.

[$(Cp^*Ta)_2B_5H_{11}$] (**2**): $C_{20}H_{41}B_5Ta_2$, triclinic, $P\bar{1}$, $a$ = 8.8827(4), $b$ = 11.8488(5), $c$ = 12.0608(5) Å, $\alpha$ = 71.640(4), $\beta$ = 85.455(3), $\gamma$ = 88.886(3)°, $Z$ = 2, $\rho_{calcd}$ = 1.929 Mg m$^{-3}$, final $R$ indices [$I > 2\sigma(I)$] $R_1$ = 0.0357, $wR_2$ = 0.0806, index ranges $-10 \le h \le 10$, $-14 \le k \le 14$, $-14 \le l \le 14$, crystal size 0.25 × 0.12 × 0.05 mm, reflections collected 10305, independent reflections 4217, ($R$(int) = 0.0227), GOF on $F^2$ 1.101.

[{$Cp^*Ta$}$_2B_5H_{10}(C_6H_4CH_3)$] (**3**): The intensity data were collected by $\omega$–$\phi$ scan with frame width of 0.5°. Frame integration and data reduction were performed with Brukker SAINT-plus (Version 7.06a) software. A multiscan absorption correction was applied to the data by using SADABS (Bruker AXS, **1999**) software. $C_{27}H_{46}B_5Ta_2$, triclinic, $P\bar{1}$, $a$ = 8.6670(17), $b$ = 10.059(2), $c$ = 17.793(4) Å, $\alpha$ = 81.82(3), $\beta$ = 81.81(3), $\gamma$ = 75.49(3)°, $Z$ = 2, $\rho_{calcd}$ = 1.768 Mg m$^{-3}$, final $R$ indices [$I > 2\sigma(I)$] $R_1$ = 0.0459, $wR_2$ = 0.1111, index ranges $-10 \le h \le 10$, $-11 \le k \le 11$, $-21 \le l \le 21$, crystal size 0.05 × 0.05 × 0.05 mm, reflections collected 26766, independent reflections 5169, ($R$(int) = 0.0532), GOF on $F^2$ 1.142.

[$(Cp^*TaCl)_2B_5H_{11}$] (**4**): $C_{20}H_{41}B_5Cl_2Ta_2$, monoclinic, $P2_1/n$, $a$ = 8.07310(10), $b$ = 15.1442(3), $c$ = 21.0979(4) Å, $\beta$ = 98.216(2)°, $Z$ = 4, $\rho_{calcd}$ = 1.999 Mg m$^{-3}$, final $R$ indices [$I > 2\sigma(I)$] $R_1$ = 0.0270, $wR_2$ = 0.0633, index ranges $-9 \le h \le 9$, $-18 \le k \le 17$, $-16 \le l \le 25$, crystal size 0.25 × 0.22 × 0.18 mm$^3$, reflections collected 14279, independent reflections 4491, ($R$(int) = 0.0234), GOF on $F^2$ 1.048.

CCDC-680860 (**1**), CCDC-680861 (**2**), CCDC-680862 (**3**), and CCDC-680863 (**4**) contain the supplementary crystallographic data for this paper. These data can be obtained free of charge from The Cambridge Crystallographic Data Centre via www.ccdc.cam.ac.uk/data_request/cif.

## Acknowledgements

Generous support of the Department of Science and Technology, DST (Project No. SR/S1/IC-19/2006) and the Council of Scientific and Industrial Research (CSIR), New Delhi is gratefully acknowledged. We thank Prof. N. Chandrakumar and co-workers for skilful technical assistance with the NMR experiments. S.K.B. thanks the University Grants Commission, India for a Junior Research Fellowship.

---

[1] T. P. Fehlner, J.-F. Halet, J.-Y. Saillard, *Molecular Clusters. A Bridge to Solid-State Chemistry*, Cambridge University Press, Cambridge, **2007**.

[2] a) N. N. Greenwood, I. M. Ward, *Chem. Soc. Rev.* **1974**, *3*, 231–271; b) R. N. Grimes, *Acc. Chem. Res.* **1978**, *11*, 420–427; c) R. N. Grimes, *Pure Appl. Chem.* **1982**, *54*, 43–58; d) R. N. Grimes in *Metal Interactions with Boron Clusters* (Ed.: R. N. Grimes), Plenum, New York, **1982**, pp. 269–319.

[3] a) J. D. Kennedy, *Prog. Inorg. Chem.* **1984**, *32*, 519–670; b) J. D. Kennedy, *Prog. Inorg. Chem.* **1986**, *34*, 211–434; c) J. D. Kennedy in *Disobedient Skeletons* (Ed.: J. Casanova), Wiley, New York, **1998**.

[4] D. F. Gaines in *Recent Advances in the Chemistry of Pentaborane(9)* (Eds.: R. W. Parry, G. Kodama), Pergamon, Oxford, **1980**.

[5] a) L. Barton, D. K. Srivastava in *Comprehensive Organometallic Chemistry II, Vol. 1* (Eds.: E. Abel, F. G. A. Stone, G. Wilkinson), Pergamon, New York, **1995**, Chap. 8; b) R. N. Grimes in *Comprehensive Organometallic Chemistry II, Vol. 1* (Eds.: E. Abel, F. G. A. Stone, G. Wilkinson), Pergamon, New York, **1995**, Chap. 9.

[6] a) S. J. Hildebrandt, D. F. Gaines, J. C. Calabrese, *Inorg. Chem.* **1978**, *17*, 790–794; b) S. G. Shore, D.-Y. Jan, L.-Y. Hsu, W.-L. Hsu, *J. Am. Chem. Soc.* **1983**, *105*, 5923–5924; c) D.-Y. Jan, D. P. Workman, L.-Y. Hsu, J. A. Krause, S. G. Shore, *Inorg. Chem.* **1992**, *31*, 5123–5131; d) T. J. Coffy, G. Medford, J. Plotkin, G. J. Long, J. C. Huffman, S. G. Shore, *Organometallics* **1989**, *8*, 2404–2409; e) T. J. Coffy, S. G. Shore, *J. Organomet. Chem.* **1990**, *394*, C27-C30.

[7] a) J. J. Briguglio, L. G. Sneddon, *Organometallics* **1985**, *4*, 721–726; b) D. E. Kadlecek, P. J. Carroll, L. G. Sneddon, *J. Am. Chem. Soc.* **2000**, *122*, 10868–10877; c) R. P. Micciche, P. J. Carroll, L. G. Sneddon, *Organometallics* **1985**, *4*, 1619–1623.

[8] R. N. Leyden, B. P. Sullivan, R. T. Baker, M. F. Hawthorne, *J. Am. Chem. Soc.* **1978**, *100*, 3758–3765.

[9] H.-J. Yao, C.-H. Hu, J. Sun, R.-S. Jin, P.-J. Zheng, J. Bould, R. Greatrex, J. D. Kennedy, D. L. Ormsby, M. Thornton-Pett, *Collect. Czech. Chem. Commun.* **1999**, *64*, 927–929.

[10] Y.-H. Kim, P. A. Cooke, R. Greatrex, J. D. Kennedy, M. Thornton-Pett, *J. Organomet. Chem.* **1998**, *550*, 341–345.

[11] R. H. Crabtree, *The Organometallic Chemistry of the Transition Metals*, 2nd ed., Wiley, New York, **1994**.

[12] C. E. Housecroft, T. P. Fehlner, *Adv. Organomet. Chem.* **1982**, *21*, 57.

[13] Chromium: a) J. Ho, K. J. Deck, Y. Nishihara, M. Shang, T. P. Fehlner, *J. Am. Chem. Soc.* **1995**, *117*, 10292–10299; b) S. Aldridge, H. Hashimoto, K. Kawamura, M. Shang, T. P. Fehlner, *Inorg. Chem.* **1998**, *37*, 928–940.

[14] Molybdenum: S. Aldridge, M. Shang, T. P. Fehlner, *J. Am. Chem. Soc.* **1998**, *120*, 2586–2598.

[15] Tungsten: A. S. Weller, M. Shang, T. P. Fehlner, *Organometallics* **1999**, *18*, 53–64.

[16] Rhenium: a) A. S. Weller, M. Shang, T. P. Fehlner, *Chem. Commun.* **1998**, 1787–1788; b) S. Ghosh, M. Shang, T. P. Fehlner, *J. Organomet. Chem.* **2000**, *614–615*, 92–98.

[17] Ruthenium: a) X. Lei, M. Shang, T. P. Fehlner, *Inorg. Chem.* **1998**, *37*, 3900–3901; b) X. Lei, M. Shang, T. P. Fehlner, *J. Am. Chem. Soc.* **1999**, *121*, 1275–1287.

[18] Cobalt: Y. Nishihara, K. J. Deck, Y. Nishihara, M. Shang, T. P. Fehlner, B. S. Haggerty, A. L. Rheingold, *Organometallics* **1994**, *13*, 4510–4522.

[19] Rhodium: X. Lei, M. Shang, T. P. Fehlner, *J. Am. Chem. Soc.* **1998**, *120*, 2686–2687.

[20] Iridium: X. Lei, M. Shang, T. P. Fehlner, *Chem. Eur. J.* **2000**, *6*, 2653–2664.

[21] Vanadium: D. Y. Kim, G. S. Girolami, *J. Am. Chem. Soc.* **2006**, *128*, 10969–10977; Niobium: P. D. Grebenik, J. B. Leach, J. M. Pounds, M. L. H. Green, P. Mountford, *J. Organomet. Chem.* **1990**, *382*, C1-C5; tantalum: a) F. A. Cotton, L. M. Daniels, C. A. Murillo, X. Wang, *J. Am. Chem. Soc.* **1996**, *118*, 4830–4833; b) F. A. Cotton, C. A. Murillo, X. Wang, *J. Am. Chem. Soc.* **1998**, *120*, 9594–9599. See also refs. [22,23].

[22] C. Ting, L. Messerle, *J. Am. Chem. Soc.* **1989**, *111*, 3449–3450.

[23] S. Aldridge, H. Hashimoto, M. Shang, T. P. Fehlner, *Chem. Commun.* **1998**, 207–208.

[24] D. M. P. Mingos, D. J. Wales, *Introduction to Cluster Chemistry*, Prentice Hall, New York, **1990**.

[25] a) K. Wade, *Adv. Inorg. Chem. Radiochem.* **1976**, *18*, 1–66; b) D. M. P. Mingos, *Nat. Phys. Sci.* **1972**, *239*, 16–26.

[26] N. P. Rath, T. P. Fehlner, *J. Am. Chem. Soc.* **1988**, *110*, 5345–5349.

[27] A. S. Weller, T. P. Fehlner, *Organometallics* **1999**, *18*, 447–450.

[28] The Mo compound was described earlier with $\eta^5$-$C_5H_4Me$ ligands: H. J. Bullick, P. D. Grenbenik, M. L. H. Green, A. K. Hughes, J. B. Leach, P. C. McCowan, *J. Chem. Soc. Dalton Trans.* **1995**, 67–75.

[29] B. L. Guennic, H. Jiao, S. Kahlal, J.-Y. Saillard, J.-F. Halet, S. Ghosh, A. M. Beatty, A. L. Rheingold, T. P. Fehlner, *J. Am. Chem. Soc.* **2004**, *126*, 3203–3217.

[30] P. A. Belmonte, R. R. Schrock, C. S. Day, *J. Am. Chem. Soc.* **1982**, *104*, 3082–3089.

[31] a) J. E. Huheey, *Inorganic Chemistry. Principles of Structure and Reactivity*, Harper and Row, New York, **1972**; b) F. A. Cotton, G. Wilkinson, C. A. Murillo, M. Bochmann, *Advanced Inorganic Chemistry*, 6th ed., Wiley, New York, **1999**.

[32] a) M. R. Churchill, H. J. Wasserman, *Inorg. Chem.* **1982**, *21*, 226–230; b) G. C. Campbell, J. A. M. Canich, F. A. Cotton, S. A. Duraj, J. F. Haw, *Inorg. Chem.* **1986**, *25*, 287–290; c) P. A. Belmonte, F. G. N. Cloke, R. R. Schrock, *J. Am. Chem. Soc.* **1983**, *105*, 2643–2650.

[33] a) M. R. Churchill, S. A. Julis, *Inorg. Chem.* **1977**, *16*, 1488–1494; b) M. R. Churchill, S. W. -Y. Ni, *J. Am. Chem. Soc.* **1973**, *95*, 2150–2155.

[34] a) A. P. Sattelberger, Jr., R. B. Wilson, J. C. Huffman, *Inorg. Chem.* **1982**, *21*, 4179–4184; b) P. Belmonte, R. R. Schrock, M. R. Churchill, W. J. Youngs, *J. Am. Chem. Soc.* **1980**, *102*, 2858–2860.

[35] R. Poli, *Chem. Rev.* **1991**, *91*, 509–551.

[36] S. K. Bose, S. Ghosh, B. C. Noll, J.-F. Halet, J. -Y. Saillard, A. Vega, *Organometallics* **2007**, *26*, 5377–5385.

[37] a) S. Ghosh, A. M. Beatty, T. P. Fehlner, *Angew. Chem.* **2003**, *115*, 4826–4828; *Angew. Chem. Int. Ed.* **2003**, *42*, 4678–4680; b) S. Ghosh, B. C. Noll, T. P. Fehlner, *Angew. Chem.* **2005**, *117*, 2976–2978; *Angew. Chem. Int. Ed.* **2005**, *44*, 2916–2918.

[38] G. E. Ryschkewitsch, K. C. Nainan, *Inorg. Synth.* **1975**, *15*, 113–114.

Received: March 16, 2008
Revised: July 3, 2008